

Volume Title

ASP Conference Series, Vol. **Volume Number**

Author

© **Copyright Year** Astronomical Society of the Pacific

Spitzer Mid-Infrared Photometry of 500 – 750 K Brown Dwarfs

S. K. Leggett¹, L. Albert², E. Artigau³, Ben Burningham⁴, X. Delfosse⁵, P. Delorme⁶, T. Forveille⁵, P. W. Lucas⁴, M. S. Marley⁷, D. J. Pinfield⁴, C. Reylé⁸, D. Saumon⁹, R. L. Smart¹⁰, and S. J. Warren¹¹

¹*Gemini Observatory Northern Operations, 670 N. A’ohoku Place, Hilo, Hawaii 96720, USA*

²*Canada-France-Hawaii Telescope, 65-1238 Mamalahoa Highway, Kamuela, Hawaii 96743, USA*

³*Département de Physique and Observatoire du Mont Mégantic, Université de Montréal, C.P. 6128, Succursale Centre-Ville, Montréal, QC H3C 3J7, Canada*

⁴*Centre for Astrophysics Research, Science and Technology Research Institute, University of Hertfordshire, Hatfield AL10 9AB, UK*

⁵*Laboratoire d’Astrophysique de Grenoble, Université J. Fourier, CNRS, UMR5571, Grenoble, France*

⁶*School of Physics and Astronomy, University of St Andrews, North Haugh, St Andrews KY16 9SS, United Kingdom*

⁷*NASA Ames Research Center, Mail Stop 245-3, Moffett Field, CA 94035, USA*

⁸*Besançon Observatory, Université de Franche-Comté, Institut Utinam, UMR CNRS 6213, BP 1615, 25010 Besançon Cedex, France*

⁹*Los Alamos National Laboratory, P.O. Box 1663, MS F663, Los Alamos, NM 87545, USA*

¹⁰*INAF/Osservatorio Astronomico di Torino, Strada Osservatorio 20, 10025 Pino Torinese, Italy*

¹¹*Imperial College London, Blackett Laboratory, Prince Consort Road, London SW7 2AZ, UK*

Abstract. Mid-infrared data, including *Spitzer* warm-IRAC [3.6] and [4.5] photometry, is critical for understanding the cold population of brown dwarfs now being found, objects which have more in common with planets than stars. As effective temperature (T_{eff}) drops from 800 K to 400 K, the fraction of flux emitted beyond $3\ \mu\text{m}$ increases rapidly, from about 40% to >75%. This rapid increase makes a color like $H-[4.5]$ a very sensitive temperature indicator, and it can be combined with a gravity- and metallicity-sensitive color like $H - K$ to constrain all three of these fundamental properties, which in turn gives us mass and age for these slowly cooling objects. Determination of mid-infrared color trends also allows better exploitation of the WISE mission by the community. We use new *Spitzer* Cycle 6 IRAC photometry, together with published data, to present trends of color with type for L0 to T10 dwarfs. We also use the atmospheric and evolutionary models of Saumon & Marley to investigate the masses and ages of 13 very late-type T dwarfs, which have $H-[4.5] > 3.2$ and $T_{\text{eff}} \approx 500\ \text{K}$ to 750 K.

Note: This is an updated version of Leggett et al. (2010a); a photometry compilation is available at www.gemini.edu/staff/sleggett.

1. Introduction

The last decade has seen a remarkable increase in our knowledge of the bottom of the stellar main-sequence and of the low-mass stellar and sub-stellar (brown dwarf) population of the solar neighborhood. Two classes have been added to the spectral type sequence following M — L, and T; T dwarfs with effective temperatures (T_{eff}) as low as 500 K are now known and we are truly finding objects that provide the link between the low-mass stars and the giant planets. As T_{eff} decreases, brown dwarfs emit significant flux at mid-infrared wavelengths (e.g. Burrows et al. 2003; Leggett et al. 2009). At $T_{\text{eff}} = 1000$ K 30% of the total flux is emitted at wavelengths longer than $3 \mu\text{m}$, while at 600 K 60% of the flux is emitted in this region (according to our models).

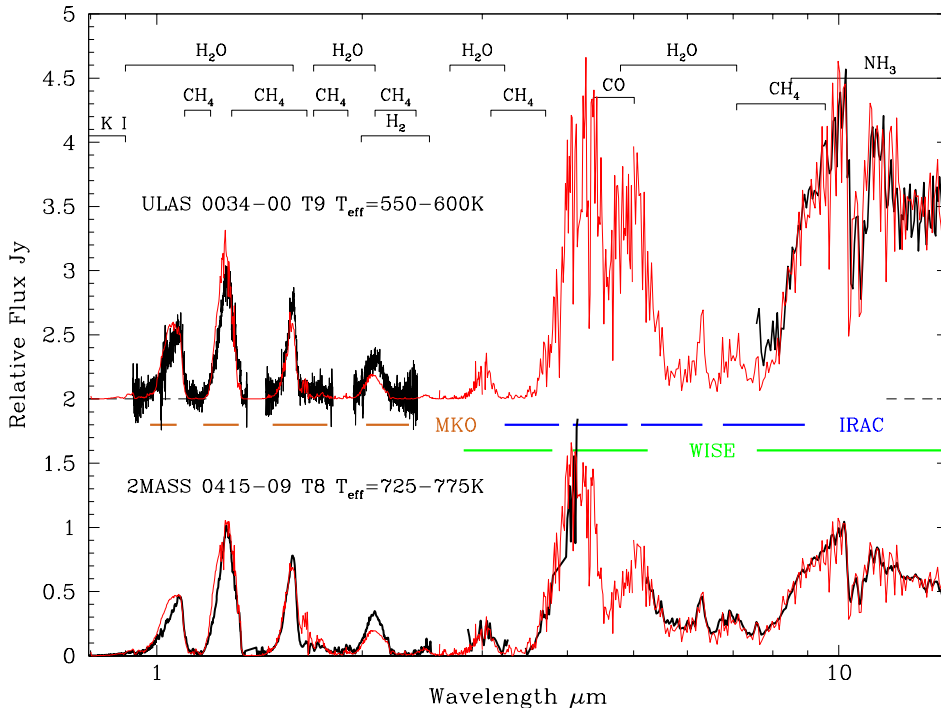


Figure 1. Observed (black lines) and modelled (red lines) SEDs of the 750 K T8 dwarf 2MASS 0415-09 (lower spectrum, Saumon et al. 2007), and the 600 K T9 dwarf ULAS 0034-00 (upper spectrum, Leggett et al. 2009). Principal absorption features are identified; NH₃ is also likely for the T9 dwarf near 1.0, 1.2, 1.3, 1.5 and 1.8 μm . The MKO-system *YJHK*, IRAC and WISE filter bandpasses are indicated.

Figure 1 shows spectral energy distributions (SEDs) for a 750 K T8 dwarf and a 600 K T9 dwarf; the flux emerges from windows between strong bands of, primarily, CH₄ and H₂O absorption. As the temperature drops from 750 K to 600 K, the ratio of the mid- to the near-infrared flux increases dramatically, and more flux emerges through

the windows centered near $5\ \mu\text{m}$ and $10\ \mu\text{m}$. Filter passbands are indicated for the near-infrared *YJHK* MKO-system (Tokunaga et al. 2002), as well as the *Spitzer* IRAC bands (Fazio et al. 2004) and the three shortest-wavelength WISE bands (Liu et al. 2008). The IRAC and WISE filters sample regions of both high and low flux, thus both cameras are sensitive to cold brown dwarfs, which can be identified by extreme colors in their respective photometric systems.

We used *Spitzer* Cycle 6 time to obtain IRAC photometry of late-type T dwarfs. Here we combine these data with published photometry to examine trends in colors with spectral type, which will be useful for the design and use of ongoing and planned infrared surveys. We also examine in detail the colors of the $500 \leq T_{\text{eff}} \text{ K} \leq 800$ dwarfs for correlations with the photospheric parameters effective temperature, gravity, and metallicity. We find that various colors do provide indicators of temperature and gravity, which in turn constrains mass and age when combined with evolutionary models.

2. Trends with Type, and Survey Sensitivities

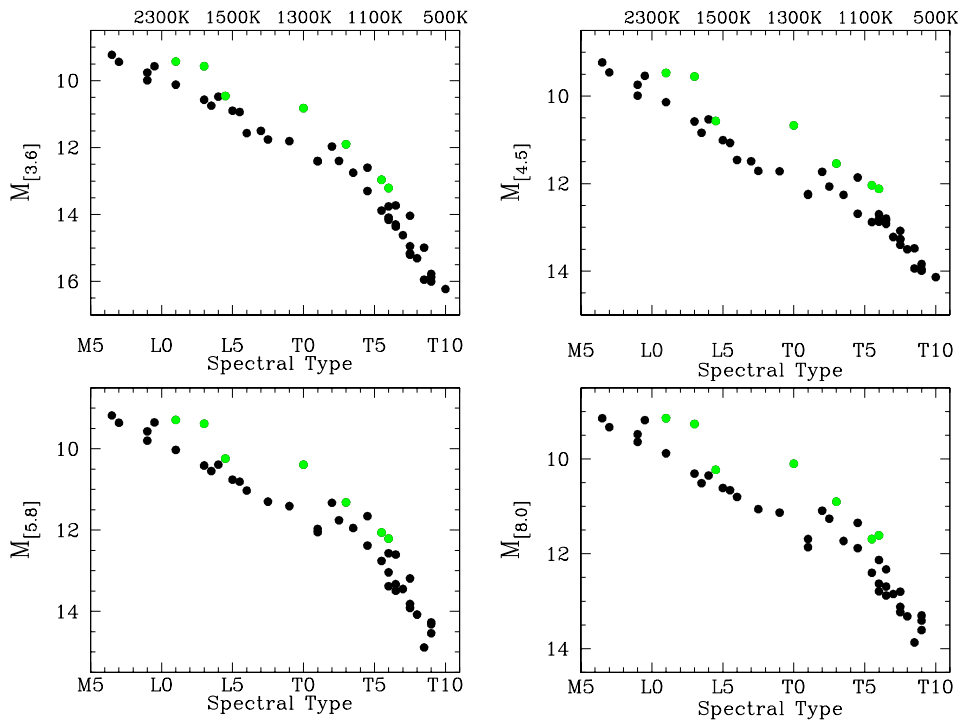


Figure 2. Absolute IRAC magnitudes as a function of spectral type; infrared spectral type is used for both L and T dwarfs and the uncertainty is 0.5 - 1.0 subclass. Green points are known binary systems. T_{eff} values on the top axes are from the Stephens et al. (2009) empirical T_{eff} :type relationship.

Figure 2 shows absolute IRAC [3.6], [4.5], [5.8] and [8.0] magnitudes as a function of spectral type. For the latest-type T dwarfs, because of the redistribution of the flux to the mid-infrared, the drop in intrinsic brightness at these wavelengths is much less than in the near-infrared. At *YJHK* there is an increase of 4 to 5 magnitudes from

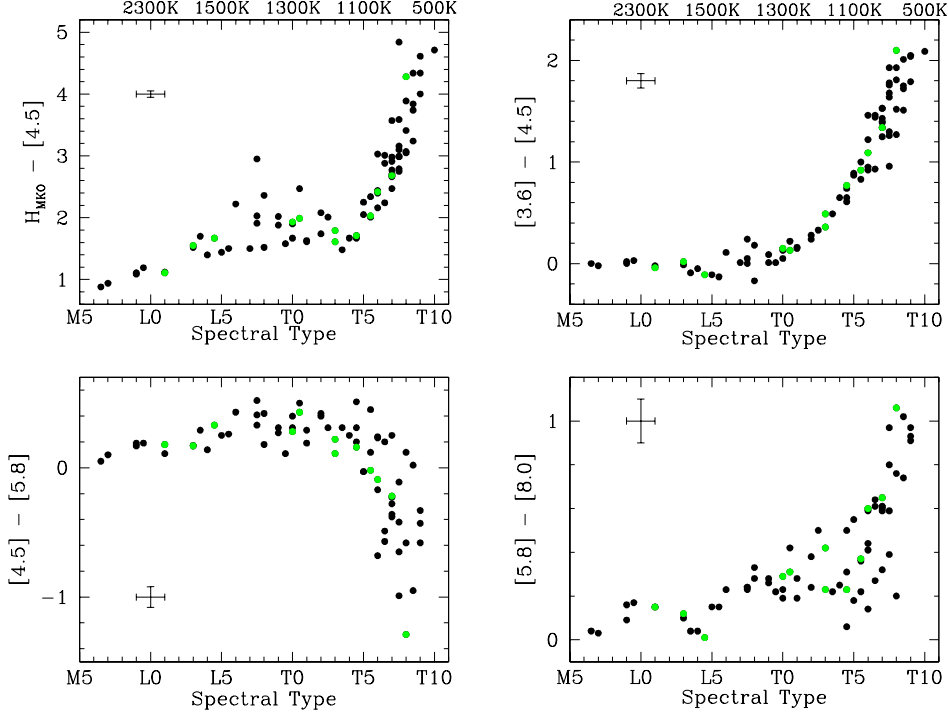


Figure 3. IRAC colors as a function of spectral type; infrared spectral type is used for both L and T dwarfs. Green points are known binary systems. Typical uncertainties are indicated. T_{eff} values on the top axes are from the Stephens et al. (2009) empirical T_{eff} :type relationship.

T5 to T10, as opposed to the ~ 2 magnitudes shown in Figure 2. This means that the mid-infrared all-sky mission WISE is ideally suited for detecting the very cold brown dwarfs. Assuming that the mass function is flat (e.g. Burningham et al. 2010a), and using the simulations by Burgasser (2004), we estimate that WISE will find forty-five 500 K and thirty 400 K brown dwarfs (using the sensitivities in Mainzer et al. 2005).

Figure 3 shows various colors as a function of type. T5 and later types become rapidly redder in [3.6]-[4.5] and [5.8]-[8.0], but bluer in [4.5]-[5.8]. The dispersion for these types is relatively small compared to the photometric uncertainties. Some scatter however is seen in [4.5]-[5.8], most likely due to variations in the CO absorption, which impacts the [4.5] flux and which is gravity- and metallicity-sensitive.

3. Temperature, Metallicity and Gravity

We now examine observed and modeled trends for the coolest dwarfs in our sample. The color $H-[4.5]$ is a sensitive indicator of T_{eff} for late-type T dwarfs (Warren et al. 2007; Stephens et al. 2009; Leggett et al. 2010a). Here, we select dwarfs with $H-[4.5] > 3.2$, which produces a sample cooler than ~ 800 K. Thirteen objects fall into this category, and are listed in Table 1. Figure 4 shows $H-K$ and [4.5]-[5.8] as a function of $H-[4.5]$, and Figure 5 shows M_H and $M_{[4.5]}$ as a function of $H-K$, $H-[4.5]$ and [4.5]-[5.8]. Note that [5.8] photometry is not available for dwarfs observed in the post-

cryogenic *Spitzer* mission. Model sequences with a range of gravity and metallicity are also shown (Marley et al. 2002; Saumon & Marley 2008).

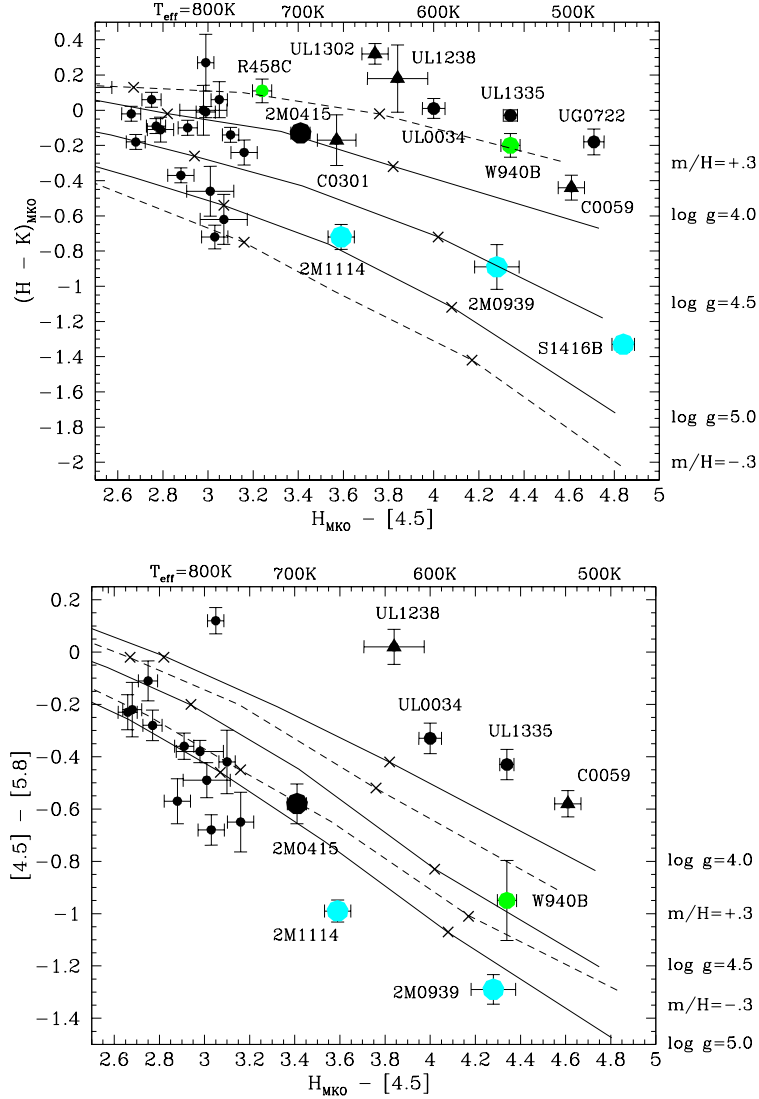


Figure 4. Temperature-sensitive $H-[4.5]$ against gravity- and metallicity-sensitive $H - K$ (top) and $[4.5]-[5.8]$ (bottom); dwarfs with $H-[4.5] > 3.2$ are identified and studied in detail. For these objects, symbol color indicates metallicity: black is unknown, green is solar, and cyan is metal-poor. Size indicates gravity: largest to smallest filled circles have $\log g > 5$, ~ 5.0 and ~ 4.5 ; triangles have unconstrained gravity. Model sequences with $\log g = 4.0, 4.5$ and 5.0 and $[m/H]=0$ are shown as solid lines, and $\log g = 4.5$ with $[m/H]= -0.3$ and $+0.3$ as dashed lines. Crosses indicate the locations along the sequences of the $T_{\text{eff}} = 800\text{ K}$ and 600 K points.

Some of these objects are well-studied, and we indicate in the figures metallicity and gravity where these are known; these and other parameters are listed in Table 1.

Table 1. Sample of Very Late-Type T Dwarfs with $H-[4.5] > 3.2$.

Name	Spectral Type	T_{eff} (K)	$\log g$	[m/H]	Mass (Jupiter)	Age (Gyr)	References ^a	
							A	B
CFBDS 0301-16	T7	700 - 750	~ 5.0	~ 0.0	20 - 40	0.4 - 4.0	1	2
2MASS 1114-26	T7.5	725 - 775	5.0 - 5.3	-0.3	30 - 50	3 - 8	3	4
SDSS 1416+13B	T7.5	500 - 700	4.8 - 5.6	≤ -0.3	20 - 45	2 - 10	5, 6	5, 7
2MASS 0415-09	T8	725 - 775	5.0 - 5.4	≥ 0	33 - 58	3 - 10	8	9
2MASS 0939-24	T8	500 - 700	5.0 - 5.3	-0.3	20 - 40	2 - 10	3	10
Ross 458C	T8.5	700 - 750	~ 4.5	0.0	7 - 20	0.1 - 1.0	11	2
Wolf 940B	T8.5	585 - 625	4.8 - 5.2	0.1	24 - 45	3 - 10	12	13
ULAS 1302+13	T8.5	650 - 700	4.0 - 4.5	> 0	5 - 15	0.1 - 0.4	14	2
ULAS 1238+09	T8.5	575 - 625	4.0 - 4.5	≥ 0	6 - 10	0.2 - 1.0	15	16
CFBDS 0059-01	T9	500 - 550	4.5 - 5.0	~ 0	10 - 30	1 - 10	17	2
ULAS 0034-00	T9	550 - 600	4.5	≥ 0	13 - 20	1 - 2	18	19
ULAS 1335+11	T9	500 - 550	4.5	≥ 0	5 - 20	0.1 - 2	15	10
UGPS 0722-05	T10	480 - 560	4.0 - 4.5	~ 0	5 - 15	0.2 - 2.0	20	20

^a References are to discovery (A) and parameter derivation (B). (1) Reyl e et al. (2010); (2) this work; (3) Tinney et al. (2005); (4) Leggett et al. (2007); (5) Burningham et al. (2010b); (6) Scholz (2010); (7) Burgasser et al. (2010); (8) Burgasser et al. (2002); (9) Saumon et al. (2007); (10) Leggett et al. (2009); (11) Goldman et al. (2010); (12) Burningham et al. (2009); (13) Leggett et al. (2010b); (14) Burningham et al. (2010a); (15) Burningham et al. (2008); (16) Leggett et al. (2010a); (17) Delorme et al. (2008); (18) Warren et al. (2007); (19) Smart et al. (2010); (20) Lucas et al. (2010).

It can be seen that, while there is not exact agreement between models and data, the general trends are reproduced, with metal-poor and high-gravity dwarfs being blue in $H - K$ and $[4.5]-[5.8]$, and slightly redder in $H-[4.5]$. The $H - K$ color is impacted by pressure-induced H_2 opacity which is sensitive to metallicity and to a lesser extent gravity. The $[4.5]$ flux is impacted by a gravity- and metallicity-sensitive CO band. There is degeneracy between the effects of gravity and metallicity, but there is an indication that $H - K$ is more sensitive to metallicity and $[4.5]-[5.8]$ to gravity, as the models calculate. The location of the dwarfs in Figures 4 and 5 relative to benchmark dwarfs, allows temperature, metallicity and gravity to be newly estimated for four dwarfs, and these parameters are given in Table 1. Note that these values do not rely on the absolute values implied by the models, but instead the models are used in a relative sense, using well-studied dwarfs as benchmarks.

4. Conclusions

The IRAC data implies that the majority of the UKIDSS 500 K to 600 K dwarfs are young and low mass, a result not currently understood in terms of selection effects or the mass function. Photometric data at wavelengths longer than $3 \mu\text{m}$ are both important and useful for the latest-type T dwarfs with $500 \leq T_{\text{eff}} \text{ K} \leq 800$, and will be even more so for the cooler objects expected to be found by WISE and other sky surveys. It is only possible to get such data from the ground for very bright objects and mid-infrared space missions are crucial for continued progress in this field.

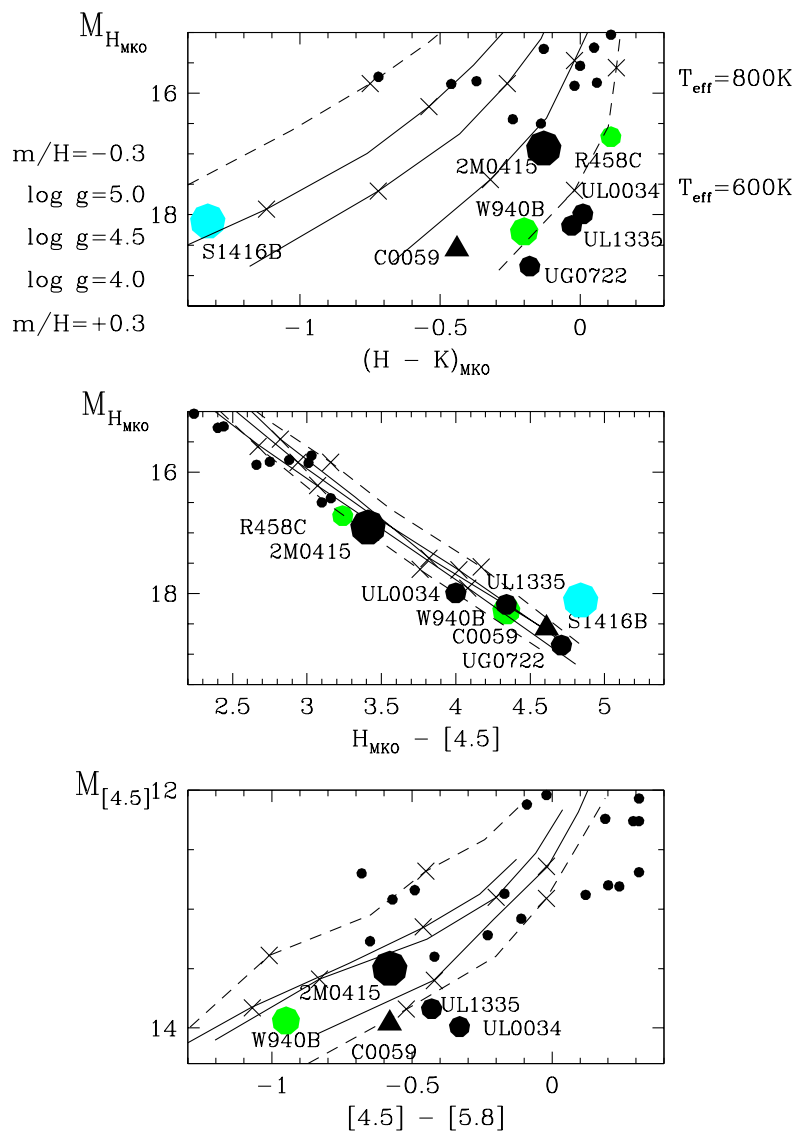


Figure 5. Absolute H and $[4.5]$ magnitudes as a function of various colors. Symbols and line types are as in Figure 4.

Acknowledgments. This work is based on observations made with the *Spitzer* Space Telescope, which is operated by the Jet Propulsion Laboratory, California Institute of Technology under a contract with NASA. Support for this work was provided by NASA through an award issued by JPL/Caltech. Support for this work was also provided by the *Spitzer* Space Telescope Theoretical Research Program, through NASA. SKL's research is supported by the Gemini Observatory, which is operated by the Association of Universities for Research in Astronomy, Inc., on behalf of the international

Gemini partnership of Argentina, Australia, Brazil, Canada, Chile, the United Kingdom, and the United States of America.

References

- Burgasser, A. 2004, *ApJS*, 155, 191
Burgasser, A.,Looper, D., & Rayner, J. T. 2010, *AJ*, 139, 2448
Burgasser, A., et al. 2002, *ApJ*, 564, 421
Burningham, B., et al. 2008, *MNRAS*, 391, 320
— 2009, *MNRAS*, 395, 1237
— 2010a, *MNRAS*, 406, 1885
— 2010b, *MNRAS*, 404, 1952
Burrows, A., Sudarsky, D., & Lunine, J. I. 2003, *ApJ*, 596, 587
Delorme, P., et al. 2008, *A&A*, 482, 961
Fazio, G. G., et al. 2004, *ApJS*, 154, 10
Goldman, B., et al. 2010, *MNRAS*, 405, 1140
Leggett, S. K., et al. 2007, *ApJ*, 667, 537
— 2009, *ApJ*, 695, 1517
— 2010a, *ApJ*, 710, 1627
— 2010b, *ApJ*, 720, 252
Liu, F., et al. 2008, in *Modeling, Systems Engineering, and Project Management for Astronomy III*, edited by M. J. Angeli, George Z.; Cullum (SPIE), vol. 7017 of *Proceedings of the SPIE*, 16
Lucas, P. W., et al. 2010, *MNRAS*, 408, L56
Mainzer, A. K., et al. 2005, in *UV/Optical/IR Space Telescopes: Innovative Technologies and Concepts II*, edited by H. A. MacEwen (SPIE), vol. 5899 of *Proceedings of the SPIE*, 262
Marley, M. S., et al. 2002, *ApJ*, 568, 335
Reylé, C., et al. 2010, *A&A*, 522, 112
Saumon, D., & Marley, M. S. 2008, *ApJ*, 689, 1327
Saumon, D., et al. 2007, *ApJ*, 662, 1245
Scholz, R. D. 2010, *A&A*, 510, L8
Smart, R. L., et al. 2010, *A&A*, 511, 30
Stephens, D. C., et al. 2009, *ApJ*, 702, 154
Tinney, C. G., et al. 2005, *AJ*, 130, 2326
Tokunaga, A. T., Simons, D. A., & Vacca, W. D. 2002, *PASP*, 114, 180
Warren, S. J., et al. 2007, *MNRAS*, 381, 1400